Turbulence in a Bose-Einstein condensate of dipolar excitons in coupled quantum wells

O. L. Berman, R. Ya. Kezerashvili, G. V. Kolmakov, and Yu. E. Lozovik

Phys. Rev. B **86**, 045108 — Published 10 July 2012

DOI: 10.1103/PhysRevB.86.045108

Turbulence in a Bose-Einstein Condensate of Dipolar Excitons in Coupled Quantum Wells

O. L. Berman,[1] R. Ya. Kezerashvili,[1] G. V. Kolmakov,[1] and Yu. E. Lozovik[2]

[1]*Physics Department, New York City College of Technology, CUNY, Brooklyn, NY 11201, USA*
[2]*Institute of Spectroscopy RAS, Troitsk, Moscow region, 142190, Russia*

The nonlinear dynamics of a Bose-Einstein condensate (BEC) of dipolar excitons trapped in an external confining potential in coupled quantum wells is analyzed. It is demonstrated that under typical experimental conditions the dipolar exciton BEC can be described by a generalized Gross-Pitaevskii equation with the local interaction between the excitons, which depends on the exciton distribution function. It is shown that, if the system is pumped at sufficiently high frequencies, a steady turbulent state can be formed.

PACS numbers: 71.35.-y, 71.35.Lk, 73.21.Fg

I. INTRODUCTION

In the last decade, the nonlinear dynamics of the excitations in semiconductor heterostructures coupled with laser radiation attract attention because of promising potential applications in electronics and photonics, including, e.g., design of thresholdless lasers, optical computing and quantum computing.[1–8] One of important examples of the systems where the excitations demonstrate essentially quantum behavior is a Bose-Einstein condensate (BEC) of excitons in semiconductors.[9–14] The dynamics of dipolar excitons formed by spatially separated charges in coupled quantum wells (CQW) in semiconductor heterostructures at helium temperatures attract attention due to the relatively long exciton lifetime compared to excitons in a single quantum well.[12,13] Recently, it was also predicted that dipolar excitons can form a superfluid in a two-layer graphene.[15]

In this paper we focus on non-stationary dynamics in a dipolar exciton BEC in QCWs in an in-plane trapping potential. The trapping potential is essential for the condensate formation at finite temperatures and it can be formed in GaAs structures by applying inhomogeneous stress,[13] static electric as well as magnetic field or laser radiation (see Ref. 14 and references therein).

The dynamics of dipolar excitons is complicated thanks to long-range, $\propto 1/r^3$, interactions in the system. It was demonstrated in Refs. 16 and 17 that in the case of high enough density of the exciton gas or at high temperatures, the system can exhibit strong spatial correlations, which result in formation of quasi-crystalline or highly correlated states. Also, strong exciton-exciton interactions can lead to formation of stable biexciton complexes.[18] Below we consider the system under the conditions of the experiments[12–14] where a rarefied dipolar exciton gas of the density $n \sim 10^9 - 10^{10}$ cm^{-2} in CQW with an interwell distance $D > 0.3a_B$ at temperatures $T < T_c$ is studied ($a_B = \hbar^2/\mu_{\rm ex}e^2 \approx 14$ nm is the exciton Bohr radius, $\mu_{\rm ex}$ is the exciton reduced mass, T_c is the BEC transition temperature in the system). According to the analyses made in Refs. 16 and 18, in this particular regime the dipolar exciton gas can be considered as a quantum fluid and, in addition, the probability of biexciton formation is negligibly small. Therefore, the system can be effectively described by the Gross-Pitaevskii equation (GPE), in which the long-range exciton-exciton interaction is taken into account.

In this work, we demonstrate that under the conditions of the experiments[12–14] the interactions in a two-dimensional (2D) dipolar exciton BEC can be effectively reduced to *local interactions*. In effect, the dynamics of the BEC is described by the generalized GPE for the condensate wave function. In sharp contrast to the "standard" GPE, the effective interaction strength in the resultant equation is not constant and depends on the chemical potential of the system. Through numerical simulations based on the obtained local equations for the exciton BEC in CQW we show that, under the conditions of the resonant driving, the system can demonstrate long-lasting, non-stationary oscillations. We infer that this oscillatory state is somewhat similar to the wave turbulence observed earlier in spatially restricted nonlinear superfluid liquids.[19,20] It is important to emphasize that the dipolar exciton BEC considered below is different from an exciton polariton BEC. The extensive review of the polariton BEC properties and application of the Gross-Pitaevskii equation to this problem is presented in Ref. 21. It is known that the interaction of polaritons is local that is, all nonlocal effects, which are important for the dipolar exciton BEC dynamics, have not been considered in Ref. 21.

The paper is organized as follows. In Sec. II we consider the generalized 2D GPE and present the local approximation for a dipolar exciton BEC. The spectral representation for the generalized GPE is considered in Sec. III. The discussion of the BEC formation and the results of the numerical solution of the generalized GPE are given in Sec. IV. Finally, we summarize our conclusions in Sec. V.

II. LOCAL APPROXIMATION FOR A DIPOLAR EXCITON BEC

At temperatures much lower than the BEC transition temperature, the dynamics of a dilute dipolar exciton condensate is described by the generalized two-dimensional Gross-Pitaevskii equation

$$i\hbar\frac{\partial\Psi(\boldsymbol{r},t)}{\partial t} = -\frac{\hbar^2}{2m_{\rm ex}}\Delta\Psi(\boldsymbol{r},t) + V(\boldsymbol{r})\Psi(\boldsymbol{r},t) + \Psi(\boldsymbol{r},t) \times \int d^2\boldsymbol{r}'|\Psi(\boldsymbol{r}',t)|^2 U(\boldsymbol{r}-\boldsymbol{r}') + i\hbar\left(\hat{R}-\gamma\right)\Psi(\boldsymbol{r},t). \quad (1)$$

In Eq. (1) $\Psi(\boldsymbol{r},t)$ is the exciton condensate wave function, $m_{\rm ex}$ is the exciton mass, $V(\boldsymbol{r}) = \alpha r^2/2$ is an external parabolic trapping potential, α is the trapping potential strength, $U(\boldsymbol{r}) = e^2D^2/\varepsilon r^3$ is the pairwise exciton-exciton interaction potential, e is the electron charge, D is the interwell distance, ε is the dielectric permittivity of the semiconductor, and $\gamma = 1/2\tau_{\rm ex}$, where $\tau_{\rm ex}$ is the exciton lifetime. Below an isotropic trap is considered. However, this is not a restriction of the model and we can also consider anisotropic traps with different trapping potential strengths in x and y directions. The last term in Eq. (1) describes creation of the excitons due to the interaction with the pumping laser radiation and the exciton decay similarly to that used in earlier works.[22,23] However, to capture the resonant pumping in a given spectral domain, we introduce a linear operator $\hat{R}$ instead of the direct driving[22] or the homogenous, frequency-independent growth increment.[23] The $\hat{R}$ operator is defined via its matrix elements in a functional basis that enter into the system of equations (6) given below.

The integral term in Eq. (1) diverges at small distances that corresponds to known divergence of the scattering amplitude of the dipolar excitons.[9] To regularize this term we introduce a cutoff distance $r_0 = (\varepsilon\mu/e^2D^2)^{1/3}$ defined by the equation $U(r_0) = \mu$, where μ is the chemical potential for the exciton system. This is equivalent to the cutoff of the exciton energies at the chemical potential μ. In this case, $|\Psi(\boldsymbol{r}',t)|^2$ can be expanded in a Taylor series over $\rho = |\boldsymbol{r}-\boldsymbol{r}'|$ and the integral term reads $\int_{\rho\geq r_0} d^2\boldsymbol{r}'|\Psi(\boldsymbol{r}',t)|^2U(\rho) = g|\Psi(\boldsymbol{r},t)|^2(1 + O(r_0/a))$, where $g = 2\pi e^2D^2/\varepsilon r_0$, $O(r_0/a)$ denotes the terms of (r_0/a) order, and $a \sim \Psi(\boldsymbol{r},t)/|\nabla\Psi(\boldsymbol{r},t)|$ is the characteristic length, at which the condensate wave function changes significantly. For the low-frequency resonant driving a coincides by the order of magnitude with the size of the exciton cloud $d \sim 10$ μm.[13,14] Hence, the used approximation for the integral term is valid if $r_0 \ll 10$ μm. For the high-frequency driving, a can be smaller than d and is defined by the driving frequency. The estimates for the experimental conditions[13,14] show that $r_0/d \leq 0.04$ and therefore, the corrections $\sim (r_0/a)$ are negligible.

Thus, under the experimental conditions[13,14] the dynamics of the dipolar exciton BEC is described by the

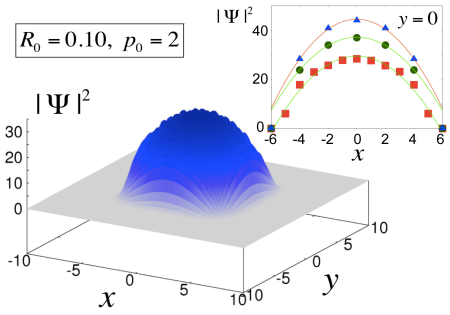

FIG. 1: (color online) Steady-state spatial distribution for the dipolar exciton BEC density in a trap for the low-frequency driving at $R_0 = 0.1$. Inset shows the evolution of the exciton density profile with rising the pumping rate R_0: 0.1 (■), 0.3 (●), and 0.5 (▲). The curves represent the Thomas-Fermi distribution function.

equation

$$i\hbar\frac{\partial\Psi(\boldsymbol{r},t)}{\partial t} = -\frac{\hbar^2}{2m_{\rm ex}}\Delta\Psi(\boldsymbol{r},t) + V(\boldsymbol{r})\Psi(\boldsymbol{r},t) + g\Psi(\boldsymbol{r},t)|\Psi(\boldsymbol{r},t)|^2 + i\hbar\left(\hat{R}-\gamma\right)\Psi(\boldsymbol{r},t). \quad (2)$$

Eq. (2) coincides with the "traditional" GPE, in which creation and decay of the particles are taken into account. However, in Eq. (2) the exciton interaction strength g depends on the chemical potential of the system and thus, on the density of the exciton BEC. In what follows we incorporate the equation for the chemical potential in the BEC determined for a dilute gas in a trap,[24]

$$\mu = (H^{(2)} + 2H^{(4)})/N, \quad (3)$$

where

$$H^{(2)} = \int d\boldsymbol{r}\left(\frac{\hbar^2}{2m_{\rm ex}}|\nabla\Psi(\boldsymbol{r},t)|^2 + |\Psi(\boldsymbol{r},t)|^2V(\boldsymbol{r})\right),$$
$$H^{(4)} = \frac{g}{2}\int d\boldsymbol{r}|\Psi(\boldsymbol{r},t)|^4, \quad (4)$$

are the quadratic and fourth-order terms in the Hamiltonian of the system and $N = (1/2)\int d\boldsymbol{r}|\Psi(\boldsymbol{r},t)|^2$ is the total number of the excitons in the BEC.

III. SPECTRAL REPRESENTATION OF THE GENERALIZED GROSS-PITAEVSKII EQUATION

To investigate the nonlinear dynamics of a dipolar exciton BEC, we solve the system (2), (3) using the spectral representation

$$\Psi(\boldsymbol{r},t) = \sum_{\boldsymbol{n}} A_{\boldsymbol{n}}(t)\varphi_{\boldsymbol{n}}(\boldsymbol{r}), \quad (5)$$

where the basis functions $\varphi_{\boldsymbol{n}}(\boldsymbol{r})$ are the eigenfunctions of the Hamiltonian for a single particle in a parabolic potential,[25] $A_{\boldsymbol{n}}(t)$ are the time-dependent coefficients of the expansion of the condensate wave function, and

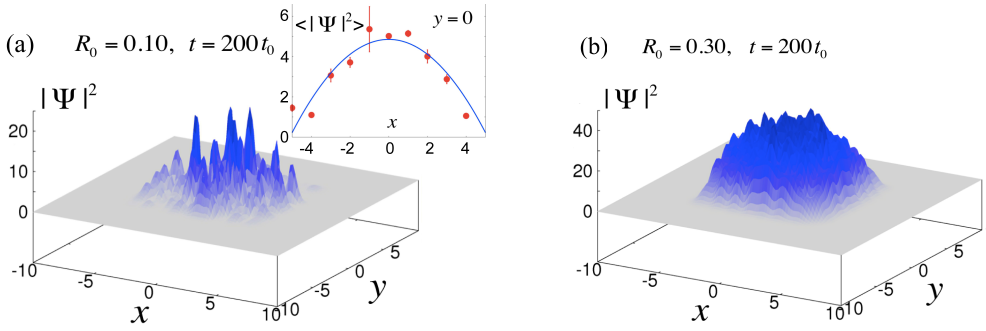

FIG. 2: (color online) The exciton density profiles at $t = 200t_0$ for (a) $R_0 = 0.1$ and (b) $R_0 = 0.3$ for the high-frequency driving at $p_1 = 4$, $p_2 = 6$. Inset on frame (a) shows the exciton density plotted at $y = 0$ and averaged over the time period $50t_0 < t < 200t_0$ and three independent runs (points). Curve shows the fitting by the Thomas-Fermi distribution.

$\boldsymbol{n} = (n_x, n_y)$ is the two-dimensional index. We will refer to the coefficients $A_{\boldsymbol{n}}(t)$ as the spectral amplitudes. The Schrödinger equation for the basis functions coincides with the linear, Hermitian part (i.e. the first two terms in the r.h.s.) of Eq. (2). This choice allows us to capture the behavior of the condensate wave function by taking into account a relatively small number of terms in the expansion for $\Psi(\boldsymbol{r}, t)$ and hence, obtain a good numerical convergence.

Substitution of the expansion (5) into Eq. (2) results in the following system of equations for the spectral amplitudes

$$\frac{\partial A_{\boldsymbol{n}}}{\partial t} = -i\omega_{\boldsymbol{n}} A_{\boldsymbol{n}} - ig \sum_{\boldsymbol{m},\boldsymbol{k},\boldsymbol{l}} W_{\boldsymbol{n},\boldsymbol{m},\boldsymbol{k},\boldsymbol{l}} A^*_{\boldsymbol{m}} A_{\boldsymbol{k}} A_{\boldsymbol{l}} + (R_{\boldsymbol{n}} - \gamma) A_{\boldsymbol{n}}, \quad (6)$$

where $\omega_{\boldsymbol{n}} = (\alpha/m_{\rm ex})^{1/2}(n_x + n_y + 1)$ is the linear oscillation frequency of the mode $A_{\boldsymbol{n}}(t)$, $W_{\boldsymbol{n},\boldsymbol{m},\boldsymbol{k},\boldsymbol{l}}$ is the matrix element of the interaction term $H^{(4)}$, and $R_{\boldsymbol{n}}$ is the matrix element of the $\hat{R}$ operator.

We numerically integrated the system of equations (6) with the 4$^{\rm th}$ order Runge-Kutta scheme on a graphical processing unit NVIDIA Tesla S2050. In the simulations, the length and time are expressed in the oscillatory units $\ell_0 = (\hbar^2/\alpha m_{\rm ex})^{1/4} = 0.9$ μm, $t_0 = (m_{\rm ex}/\alpha)^{1/2} = 1.6$ ns calculated for the external trapping potential at $\alpha = 50$ eV/cm^2 and the exciton mass $m_{\rm ex} = 0.22m_0$, where m_0 is the free electron mass. The initial conditions were chosen in the form of quasi-equilibrium distribution $A_{\boldsymbol{n}}(0) = [T/(\mu_0 + n_x + n_y + 1)]^{1/2} \exp(i\phi_{\boldsymbol{n}})$ with the dimensionless temperature $T = 0.1$, the dimensionless chemical potential $\mu_0 = 1$, and random phases $\phi_{\boldsymbol{n}}$. We found that the results only weakly depend on the choice of the T and μ_0 constants.

IV. EXCITON BEC FORMATION

We consider two cases: (a) the exciton system is pumped at low spectral modes, *i.e.*, at frequencies comparable with the fundamental frequency in the parabolic trap, $\omega_0 = t_0^{-1}$; (b) the system is pumped in the high frequency spectral domain $\omega > \omega_0$. It is worth noting that, in experiments the ratio of the driving frequency and the fundamental frequency of the trap may be tuned by changing both the laser pumping frequency and the trapping potential strength α.[13,14]

For the low-frequency driving, we set $R_{\boldsymbol{n}} = R_0$ at $n \equiv (n_x^2 + n_y^2)^{1/2} \le p_0$ where p_0 is a given cut-off and $R_{\boldsymbol{n}} = 0$ otherwise. Below, we show the results obtained for $p_0 = 2$. The driving was applied at $t = 0$. Initially, the system exhibits transient oscillations. At a later time, the oscillations were damped and the system relaxed to a stationary state, in which the spectral amplitudes $A_{\boldsymbol{n}}$ tend to constant values. The time required to approach the stationary state was equal to $t \approx 50t_0 \approx 80$ ns for a low pumping rate $R_0 = 0.1$ and it decreases to $t \approx 20t_0 \approx 32$ ns for a high pumping rate $R_0 = 0.6$. We also observed that the initial exciton distribution relaxed to zero if the pumping rate was less that the threshold value $R_0 \approx 0.03$. The presence of the finite excitation threshold is in agreement with the results of previous simulations of the polaritons dynamics.[23] Figure 1 shows the stationary non-uniform spatial distribution of the exciton BEC density at $t = 200t_0$ for $R_0 = 0.1$. It is seen in Fig. 1 that an exciton "cloud" of size $\sim 6 - 8$ ℓ_0 that is, $\sim 5 - 7$ μm is formed at the center of the trap. Formation of the cloud at the center of the trap is in agreement with the observations with indirect excitons in a trap[13] and in the BECs of trapped atomic gases.[24] It follows from the inset in Fig.1 that the spatial distribution of the exciton in the BEC can be described by the Thomas-Fermi distribution $|\Psi(\boldsymbol{r})|^2 = n_0[1 - (r/d)^2]$ (n_0 is the BEC density at the center of the trap and d is the effective radius of the cloud), which is used for characterization of inhomogeneous atomic BECs.[24] The inset in Fig. 1 demonstrates that the exciton density at the center of the trap gradually grows with the increase of the pumping rate.

When the system was driven in the high frequency spectral range ($R = R_0$ at $p_1 < n \le p_2$, and $p_2 > p_1 \ge 4$) the BEC exhibited *persistent, non-damped oscillations*. At relatively small pumping rates, $R_0 \sim 0.1$, the spatial BEC profile at any given moment of time was far from the Thomas-Fermi distribution and it was represented as

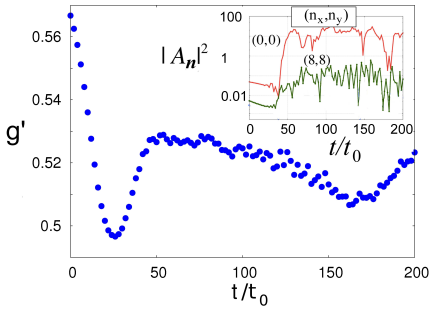

FIG. 3: (color online) Dependence of the dipolar exciton interaction strength on time for the high-frequency driving at $p_1 = 4$, $p_2 = 6$. Inset: Time dependence of the spectral amplitudes $|A_{\boldsymbol{n}}|$ at $\boldsymbol{n} = (0,0)$ (the fundamental mode) and $(8,8)$.

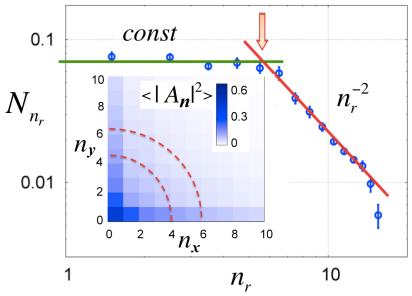

FIG. 4: (color online) Angle-averaged occupation number of the excitonic modes in the BEC, N_{n_r} as a function of the radial number n_r, plotted in log-log scale. The data are averaged over three independent runs. The center of the pumping region is labeled by a vertical arrow, $\Delta n = 3$. The lines show a power-like distribution for $N_{n_r} = const \times n_r^m$ at $m = 0$ and $m = -2$. Inset shows the averaged spectral amplitude distribution $|A_{\boldsymbol{n}}|^2$, the dashed curves show the boundaries of the pumping domain.

a series of irregular "spikes", as seen in Fig. 2a. Nevertheless, the mean exciton BEC density distribution averaged over a long enough period of time, $\langle|\Psi(\boldsymbol{r},t)|^2\rangle$, was close to the Thomas-Fermi distribution, as shown in the inset in Fig. 2a. At larger pumping rates, $R_0 \geq 0.3$, the density oscillated around a mean parabolic profile, which was close to the Thomas-Fermi distribution (Fig. 2b). We emphasize that, unlike the case of the low frequency driving, the BEC oscillations were observed during the whole time period of the simulations $200t_0$, which is much longer than the time duration of the initial transient processes. Figure 3 shows the respective oscillations of the spectral harmonics, $A_{\boldsymbol{n}}$, at $t > 50t_0$ and the variations of the dimensionless interaction strength, $g' = gm_{\rm ex}/\hbar^2$, with time. A decrease of both $A_{\boldsymbol{n}}$ and g' at $t < 50t_0$ corresponds to initial relaxation after the driving was applied.

To characterize the oscillatory regime, we plot a two-dimensional amplitude distribution $\langle|A_{\boldsymbol{n}}|^2\rangle$ averaged over time and three independent runs, as a function of (n_x, n_y), see inset in Fig. 4. It is clearly seen that, despite the system is driven at the high-frequency range (marked by dashed curves), the maximum of the spectral amplitudes (deeper color) is positioned at low spectral numbers $n \leq 2$. Therefore, mutual interaction between different spectral scales is present in the system. In other words, a flux of the excitations from the region, at which they are generated by an external pumping, toward the low-frequency region is formed. The resultant state is similar to a wave-turbulent state known for weakly nonlinear systems.[26,27] In those systems, nonlinear interaction of running waves resulted in formation of turbulence, which was characterized by establishing of power-like, Kolmogorov spectra of energy and particles distributions. In our case, the system is not spatially homogeneous and the interacting, normal variables are present by the oscillatory modes $A_{\boldsymbol{n}}$.

To further characterize the turbulent regime, we calculate the angle-averaged distribution for the spectral amplitudes, $N_{n_r} = \sum_{n=n_r}^{n_r+\Delta n}\langle|A_{\boldsymbol{n}}|^2\rangle$, Fig. 4. Formation of power-like tails of the distribution $N_{n_r} \propto n_r^m$ at frequencies below and above the characteristic driving frequency is clearly seen on the main part of Fig. 4, that supports our conclusion on the establishing of the turbulent regime in the dipolar exciton BEC in CQW. The presence of two different exponents $m = 0$ and $m = -2$ in the low- and high-frequency domains, respectively, indicates that the fluxes of the energy and of the number of particles through the scales are simultaneously formed in the system (cf. theory[26,27] for the traditional GPE).

An essential difference between the previous consideration[26,27] and our results is that (a) the interaction strength g depends on the instantaneous exciton distribution, and (b) the effective damping in the system produced by the exciton decay is finite and cannot be disregarded for all modes. As it follows from the consideration in Ref. 27, in the wave turbulent regime for the traditional GPE with the wave frequencies $\omega_{\boldsymbol{n}} \propto |\boldsymbol{n}|$ the exponents are equal to $m = -2/3$ and $m = -1$ for the low- and high-frequency spectral domains, respectively. Thus, the exponents m found in our simulations differ from those for the standard GPE. Therefore, the turbulent dynamics of the dipolar exciton BEC has different scaling properties, compared to that described by the traditional GPE.

V. CONCLUSION

In conclusion, we demonstrate that the dynamics of the Bose-Einstein condensate of dipolar excitons in coupled quantum wells can be described by the generalized Gross-Pitaevskii equation with the local (contact) interaction, despite a long-range exciton-exciton interaction is present. The effective interaction strength g is a function of the chemical potential of the system and therefore, should be determined self-consistently from the exciton distribution in the BEC. We show that, if the system is driven by an external pumping at low frequency modes, the spatial distribution of the excitons in a trap is de-

scribed well by a parabolic density profile formerly known for dilute atomic BECs. However, if the system is driven at high frequency modes, strong time-dependent density fluctuations are excited in the BEC, and the condensate density at any given moment of time can be far from the equilibrium parabolic profile. We infer that a turbulent state is formed in the exciton BEC in this case, which is characterized by a nonlocal particle balance in the system. The latter results in formation of the power-like spectra for the exciton distribution function. The turbulent state is somewhat similar to that recently observed in superfluid ^{4}He[19,20] and proposed in Ref. 28 for the atomic BEC formation. The crucial difference between all mentioned examples and the system under consideration is that in our case the interaction strength between the normal modes is a function of the occupation numbers of the modes. Therefore, turbulence can not be considered as "weak" and it involves more complex interactions between the modes. It is worth noting that formation of long-living nonequilibrium states was recently described for a classical system with long-range interaction.[29] Also, a transition to the turbulent state has been recently observed for the trapped atomic BEC in an external oscillating field.[30,31] The results of our consideration are useful for understanding of nonlinear phenomena in low-dimensional quantum systems including indirect excitons in CQW,[13,14] exciton polaritons propagation,[8] and a photon BEC in dye microcavities.[32]

Acknowledgment

The numerical computations are supported, in part, under NSF grants CNS-0958379 and CNS-0855217 and the City University of New York High Performance Computing Center at the College of Staten Island.

[1] A. H. MacDonald, P. M. Platzman, and G. S. Boebinger, Phys. Rev. Lett. **65**, 775 (1990).
[2] P. Littlewood, Science **316**, 989 (2007).
[3] A. A. High, E. E. Novitskaya, L. V. Butov, M. Hanson, and A. C. Gossard, Science **321**, 229 (2008).
[4] I. Carusotto, D. Gerace, H. E. Tureci, S. De Liberato, C. Ciuti, and A. Imamoglu, Phys. Rev. Lett. **103**, 033601 (2009).
[5] R. Johne, I. A. Shelykh, D. D. Solnyshkov, and G. Malpuech, Phys. Rev. B **81**, 125327 (2010).
[6] T. C. H. Liew and V. Savona, Phys. Rev. A **84**, 032301 (2011).
[7] D. W. Snoke, *Solid State Physics: Essential Concepts* (Addison-Wesley, San Francisco, 2009).
[8] A. Amo, T. C. H. Liew, C. Adrados, R. Houdre, E. Giacobino, A. V. Kavokin, and A. Bramati, Nat. Photonics **4**, 361 (2010).
[9] Yu. E. Lozovik and V. I. Yudson, JETP Lett. **22**, 26 (1975).
[10] X. Zhu, P. B. Littlewood, M. S. Hybertsen, and T. M. Rice, Phys. Rev. Lett. **74**, 1633 (1995).
[11] T. Fukuzawa, E. E. Mendez, and J. M. Hong, Phys. Rev. Lett. **64**, 3066 (1990).
[12] L. V. Butov, A. Zrenner, G. Abstreiter, G. Bohm, and G. Weimann, Phys. Rev. Lett. **73**, 304 (1994); L. V. Butov, C. W. Lai, A. L. Ivanov, A. C. Gossard, and D. S. Chemla, Nature **417**, 47 (2002); L. V. Butov, A. C. Gossard, and D. S. Chemla, Nature **418**, 751 (2002).
[13] D. W. Snoke, S. Denev, Y. Liu, L. Pfeiffer, and K. West, Nature **418**, 754 (2002); V. Negoita, D. W. Snoke, and K. Eberl, Phys. Rev. B **60**, 2661 (1999).
[14] A. A. High, J. R. Leonard, M. Remeika, L. V. Butov, M. Hanson, and A. C. Gossard, Nano Lett. **12**, 2605 (2012).
[15] O. L. Berman, R. Ya. Kezerashvili, and K. Ziegler, Phys. Rev. B **85**, 035418 (2012).
[16] B. Laikhtman and R. Rapaport, Europhys. Lett. **87**, 27010 (2009).
[17] Yu. E. Lozovik, UFN **179**, 309 (2009).
[18] C. Schindler and R. Zimmermann, Phys. Rev. B **78**, 045313 (2008).
[19] G. V. Kolmakov, V. B. Efimov, A. N. Ganshin, P. V. E. McClintock, and L. P. Mezhov-Deglin, Phys. Rev. Lett. **97**, 155301 (2006); A. N. Ganshin, V. B. Efimov, G. V. Kolmakov, L. P. Mezhov-Deglin, and P. V. E. McClintock, Phys. Rev. Lett. **101**, 065303 (2008).
[20] L. V. Abdurakhimov, M. Yu. Brazhnikov, I. A. Remizov, and A. A. Levchenko, JETP Lett. **91**, 271 (2010).
[21] I. Carusotto and C. Ciuti, "Quantum Fluids of Light" (2012), arXiv:1205.6500v1.
[22] A. Amo, J. Lefrere, S. Pigeon, C. Adrados, C. Ciuti, I. Carusotto, R. Houdre, E. Giacobino, and A. Bramati, Nat. Physics **5**, 805 (2009).
[23] J. Keeling and N. G. Berloff, Phys. Rev. Lett. **100**, 250401 (2008).
[24] F. Dalfovo, S. Giorgini, L. P. Pitaevskii, and S. Stringari, Rev. Mod. Phys. **71**, 463 (1999).
[25] L. D. Landau and E. M. Lifshitz, *Quantum Mechanics: Non-Relativistic Theory* (Elsevier, Oxford, 1977).
[26] D. Proment, S. Nazarenko, and M. Onorato, Phys. Rev. A **80**, 051603(R) (2009); A. Dyachenko and G. Falkovich, Phys. Rev. E **54**, 5095 (1996).
[27] V. E. Zakharov, V. S. L'vov, and G. Falkovich, *Kolmogorov Spectra of Turbulence I* (Springer, Berlin, 1992).
[28] Yu. Lvov, S. Nazarenko, and R. West, Physica D **184**, 333 (2003); V. E. Zakharov and S. V. Nazarenko, Physica D **201**, 203 (2005).
[29] F. P. C. Benetti, T. N. Teles, R. Pakter, and Y. Levin, Phys. Rev. Lett. **108**, 140601 (2012).
[30] R. F. Shiozaki, G. D. Telles, V. I. Yukalov, and V. S. Bagnato, Laser Phys. Lett. **8**, 393 (2011).
[31] J. A. Seman, E. A. L. Henn, R. F. Shiozaki, G. Roati, F. J. Poveda-Cuevas, K. M. F. Magalhaes, V. I. Yukalov, M. Tsubota, M. Kobayashi, K. Kasamatsu, and V.S. Bagnato, Laser Phys. Lett. **8**, 691 (2011).
[32] J. Klaers, J. Schmitt, T. Damm, F. Vewinger, and M. Weitz, Phys. Rev. Lett. **108**, 160403 (2012).